

Towards understanding retrosynthesis by energy-based models

Ruoxi Sun¹, Hanjun Dai², Li Li³, Steven Kearnes³, and Bo Dai²

¹Google Cloud AI ²Google Brain ³Google Research
{ruoxis, hadai, leeley, kearnes, bodai}@google.com

Abstract

Retrosynthesis is the process of identifying a set of reactants to synthesize a target molecule. It is critical to material design and drug discovery. Existing machine learning approaches based on language models and graph neural networks have achieved encouraging results. However, the inner connections of these models are rarely discussed, and rigorous evaluations of these models are largely in need. In this paper, we propose a framework that unifies sequence- and graph-based methods as energy-based models (EBMs) with different energy functions. This unified view establishes connections and reveals the differences between models, thereby enhances our understanding of model design. We also provide a comprehensive assessment of performance to the community. Additionally, we present a novel dual variant within the framework that performs consistent training to induce the agreement between forward- and backward-prediction. This model improves the state-of-the-art of template-free methods with or without reaction types.

Retrosynthesis is a critical problem in organic chemistry and drug discovery [1–5]. As the reverse process of chemical synthesis [6, 7], retrosynthesis aims to find the set of reactants that can synthesize the provided target via chemical reactions (Fig 1). Since the search space of theoretically feasible reactant candidates is enormous, models should be designed carefully to have the expression power to learn complex chemical rules and maintain computational efficiency.

Recent machine learning applications on retrosynthesis, including sequence- and graph-based models, have made significant progress [3, 8, 9]. Sequence-based models treat molecules as one-dimensional token sequences (SMILES [10], bottom of Fig 1) and formulate retrosynthesis as a sequence-to-sequence problem, where recent advances in neural machine translation [11, 12] can be applied. In this principle, the LSTM-based encoder-decoder frameworks and, more recently, transformer-based approaches have achieved promising results [13, 12, 14]. On the other hand, graph-based models have a natural representation of human-interpretable molecular graphs, where chemical rules are easily applied. Graph-based approaches that perform graph matching with templates (e.g. chemical rules) or reaction centers have reached encouraging results. Among those, G2Gs [15], RetroXpert [16] and GraphRETRO [17] outperform template-based methods by inferring reaction centers in a supervised way. In this paper, we focus on one-step retrosynthesis, which is also the foundation of multi-step retrosynthesis [3].

Our goal here is to provide a unified view of both sequence- and graph-based retrosynthesis models using an energy-based model (EBM) framework. It is beneficial because: First, the model design with EBM is very flexible. Within this framework, both types of models can be formulated as different

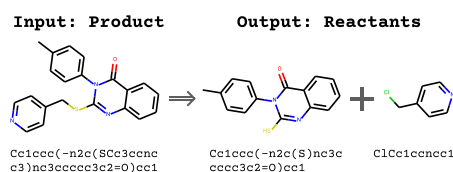


Figure 1: Retrosynthesis and SMILES.

EBM variants by instantiating the energy function into specific forms. Second, EBM provides principled ways for training models, including maximum likelihood estimator, pseudo-likelihood, etc. Third, a unified view is critical to provide insights into different EBM variants, as it is easy to extract commonalities and differences between EBM variants, understand strengths and limitations in model design, compare the complexity of learning or inference, and inspire novel EBM variants. To summarize our contributions:

- We propose a unified energy-based model (EBM) framework that integrates sequence- and graph-based models for retrosynthesis. To our best knowledge, this is the first effort to unify and exploit inner connectivity between different models.
- We perform rigorous evaluations by running tens of experiments on different model designs. Revealing the performance to the community contributes to the development of retrosynthesis models.
- Inspired by such a unified framework, we propose a novel generalized dual EBM variant that performs consistent training over forward and backward prediction directions. This model improves the state-of-the-art by 4.3%.

1 Energy-based model for Retrosynthesis

Retrosynthesis is to predict a set of reactant molecules from a product molecule. We denote the product as y , and the set of reactants predicted for one-step retrosynthesis as X . The key for retrosynthesis is to model the conditional probability $p(X|y)$. EBM provides a common theoretical framework that can unify many retrosynthesis models, including but not limited to existing models.

An EBM defines the distribution using an energy function [18, 19]. Without loss of generality, we define the joint distribution of product and reactants as follows:

$$p_{\theta}(X, y) = \frac{\exp(-E_{\theta}(X, y))}{Z(\theta)} \quad (1)$$

where the partition function $Z(\theta) = \sum_y \sum_X \exp(-E_{\theta}(X, y))$ is a normalization constant to ensure a valid probability distribution. Since the design of E_{θ} is free of choice, EBMs can be used to unify many retrosynthesis models by instantiating the energy function $E(\theta)$ with various designs. Note there is a trade-off between model expression capacity and learning tractability. EBM is also easy to obtain conditioning with different partition functions. The forward prediction probability for reaction outcome prediction $p_{\theta}(y|X)$ can be written as $\frac{\exp(-E_{\theta}(X, y))}{\sum_{y'} \exp(-E_{\theta}(X, y'))}$ with the same form of energy function.

The proposed framework works as follows: **Step 1**, design and train an energy function E_{θ} (Sec 2 and Sec 3), and **Step 2** use E_{θ} for inference in retrosynthesis (Sec 4). See Fig 2 and Algorithm 1.

2 Model Design

Based on how to parameterize reactant and product molecule X and y , the model designs can be divided into two categories: sequence-based and graph-based models.

2.1 Sequence-based Models

Here we describe several sequence-based parametrization to instantiate our EBM framework, which use SMILES string as representations of molecules. We first define the sequence-based notations.

Algorithm 1 EBM framework

[Train Phase]: Learning

Input: Reactants X and products y .

1. Parameterize X and y in *Sequence* or *Graph* format.

2. Design E_{θ} {e.g. dual, perturbed, bidirectional, graph-based, etc} // Sec 2

3. Select training loss to learn E_{θ} and obtain θ^* // Sec 3

Return θ^*

[Test Phase]: Inference // Sec 4

Input: θ^* , y^{test} , Proposal P . // Sec 4

4. Obtain a list of X candidates by P .

$L^{\text{test}} \leftarrow P(y^{\text{test}})$

5. $X^* = \arg \min_{X \in L^{\text{test}}} E_{\theta^*}(X, y^{\text{test}})$

Return: X^*

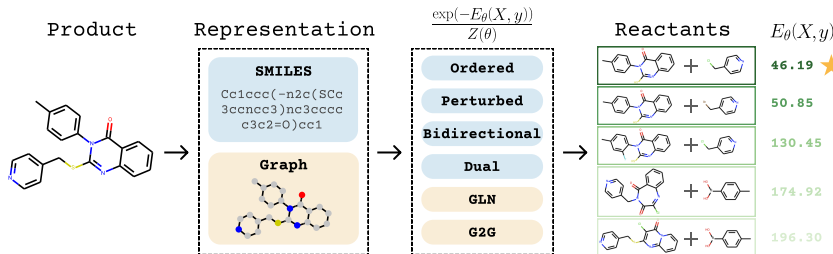


Figure 2: **EBM framework for retrosynthesis.** Given the product as input, the EBM framework (1) represents the product molecule as SMILES sequence or a graph, (2) designs and trains the energy function E_{θ} , (3) ranks reactant candidates with the trained energy score E_{θ^*} , and (4) identifies the top K reactant candidates. The best candidate has the lowest energy score (denoted by a star). The list of reactant candidates is obtained via templates (template based proposal) or directly generated by the trained model (template free proposal).

Given a reactant molecule x , we denote its SMILES representation as $s(x)$. Superscript $s(x)^{(i)}$ denotes the character at i -th position of the SMILES string. For simplicity, we use $x^{(i)}$ when possible. Reactants of a chemical reaction are usually a collection of molecules: $X = \{x_1, x_2, \dots, x_j, \dots, x_{|X|}\}$, where x_j is the j -th reactant molecule. The SMILES representation of a molecule set X , denoted as $s(X)$, is a concatenation of $s(x)$ for every x in X with “.” in between: “ $s(x_1).s(x_2)\dots s(x_{|X|})$ ”. We use $X^{(i)}$ as the short form of $s(X)^{(i)}$ to denote the i -th position of the concatenated SMILES.

2.1.1 Full energy-based model

We start by proposing a most flexible EBM that imposes the minimum restrictions on the design of E_{θ} . All the variants proposed in Sec 2.1 are special instantiations of this model (e.g. by specifying different E_{θ}). The EBM is defined as follows:

$$p(X|y) = \frac{\exp(-E_{\theta}(X, y))}{\sum_{X' \in \mathcal{P}(M)} \exp(-E_{\theta}(X', y))} \quad (2)$$

$$\propto \exp(-E_{\theta}(X, y)) \quad (3)$$

Here the energy function $E_{\theta} : \mathcal{P}(M) \times M \mapsto \mathbb{R}$ takes a molecule set and a molecule as input, and outputs a scalar value. M defines the set of all possible molecules. $\mathcal{P}(\cdot)$ represents the power set. $\mathcal{P}(M)$ denotes domain of reactant sets X . Due to the intractability of the partition function, training involves additional information e.g., template or approximation of the partition (See Sec 3).

2.1.2 Ordered model

One design of energy function is factoring the input sequence in an autoregressive manner [12, 20].

$$p_{\theta}(X|y) = \exp\left(\sum_{i=1}^{|s(X)|} \log p_{\theta}(X^{(i)}|X^{(1:i-1)}, y)\right) \quad (4)$$

$$= \exp\left(\sum_{i=1}^{|s(X)|} \log \frac{\exp(h_{\theta}(X^{(1:i-1)}, y)^{\top} e(X^{(i)}))}{\sum_{c \in S} \exp(h_{\theta}(X^{(1:i-1)}, y)^{\top} e(c))}\right) \quad (5)$$

where $p_{\theta}(X^{(i)}|X^{(1:i-1)}, y)$ is parameterized by a transformer $h_{\theta}(p, q) : S^{|p|} \times S^{|q|} \mapsto \mathbb{R}^{|S|}$ where S is vocabulary. $e(c)$ is a one-hot vector with dimension c set to 1. This choice of $h_{\theta}(p, q)$ enables efficient computing of the partition function, as it outputs a vector with length equal to $|S|$ to represent logits (unnormalized log probability) for each value in vocabulary. Here, maximum likelihood estimator (MLE) is feasible for training, as this factorization allows tractable partition function.

2.1.3 Dual model

A different design is to leverage on duality of retrosynthesis and reaction prediction. They are a pair of mutual reversible processes that factorize the joint distribution in different orders, where reaction prediction is “forward direction” – $p(y|X)$ and retrosynthesis is the “backward direction” –

$p(X|y)$. With additional prior modeling, the joint probability $p(X, y)$ factorizes to either $p(X|y)p(y)$ or $p(y|X)p(X)$. We propose a training framework that leverages on the duality of the forward and backward directions and performs consistent training between the two to bridge the divergence.

The advantage of the duality of reversible processes has been demonstrated in other applications as well. He et al. [21] trained a reinforcement learning (policy gradient) model to achieve duality in natural language processing and improved performances. Wei et al. [22] treated code summary and code generation as a pair of dual tasks, and improved efficacy by imposing symmetry between attention weights of LSTM encoder-decoder in forward and backward directions. Despite of their encouraging results, these models are not ideal for stable and efficient training for retrosynthesis, as policy gradient methods suffer from high variance and LSTM has sub-optimal performance. Therefore we propose a novel training method that is simple yet efficient for retrosynthesis task. We impose duality constraints by training forward direction on a mixture of samples drawn from the backward and original dataset. To our best knowledge, we are the first to apply duality to retrosynthesis and to impose duality constraints by samples drawn from one direction. The EBM is defined:

$$p(X|y) \propto \exp(\log p_\gamma(X) + \log p_\alpha(y|X) + \log p_\eta(X|y)) \quad (6)$$

$$= \exp(-E_\theta(X, y)) \quad (7)$$

where prior $p(X)$, forward likelihood $p(y|X)$, and backward posterior $P(X|y)$ are modeled as autoregressive models (Sec 2.1.2), parameterized by transformers with parameters γ , α , and η . Note energy function can be designed free of choice. The consistent training is achieved by minimizing the ‘‘dual loss’’, where the duality constraints in the equation below are imposed to penalize KL divergence of the two directions, *i.e.*, $\text{KL}(\text{backward}|\text{forward})$. For simplicity, we fix the backward probability in the dual loss, and therefore entropy $H(\text{backward})$ is dropped.

$$\gamma^*, \alpha^*, \eta^* = \arg \min_{\gamma, \alpha, \eta} \ell_{\text{dual}} \quad (8)$$

$$\ell_{\text{dual}} = - \left(\underbrace{\widehat{\mathbb{E}}[\log p_\gamma(X) + \log p_\alpha(y|X)]}_{\text{forward direction}} \right) \quad (9)$$

$$+ \beta \underbrace{\widehat{\mathbb{E}}_y \widehat{\mathbb{E}}_{X|y}[\log p_\gamma(X) + \log p_\alpha(y|X)]}_{\text{duality constraints}} + \underbrace{\widehat{\mathbb{E}}[\log p_\eta(X|y)]}_{\text{backward direction}} \quad (10)$$

$$= -\widehat{\mathbb{E}}_{p_{(X,y)}^{\text{mix}}}[\log p_\gamma(X) + \log p_\alpha(y|X)] - \widehat{\mathbb{E}}[\log p_\eta(X|y)] \quad (11)$$

where $\widehat{\mathbb{E}}$ indicates expectation over empirical data distribution $\hat{p}(X, y)$. The duality constraints $\beta \widehat{\mathbb{E}}_y \widehat{\mathbb{E}}_{X|y}[\log p_\gamma(X) + \log p_\alpha(y|X)]$ is the expectation of the forward direction $\log p_\gamma(X) + \log p_\alpha(y|X)$ with respect to empirical backward data distribution $\widehat{E}_y \widehat{E}_{X|y}$, where $\widehat{E}_y \widehat{E}_{X|y}$ are approximated by samples drawn from $p_\eta(X|y)$, as y is given so $p(y) = 1$. β is scale parameter. In our implementation we use size k -beam search to draw samples efficiently. Combining ‘‘forward’’ and ‘‘duality constraints’’ terms (Eq 11), we can see that the first term of the dual loss is to train the forward direction on the mixture distribution of the original data and samples drawn from backward directions $p^{\text{mix}}(X, y) = \frac{1}{1+\beta} \hat{p}(X, y) + \frac{\beta}{1+\beta} \hat{p}(y) p_\eta(X|y)$. Put every piece together (Algorithm 2

Algorithm 2 Dual Model

[Train Phase]: Learning:

Input: Reactants X and product y .

Let $\theta = \{\gamma, \alpha, \eta\}$

Define E_θ as Eq (7)

$E_\theta = \log p_\gamma(X) + \log p_\alpha(y|X) + \log p_\eta(X|y)$

1. Train backward:

$\eta^* = \arg \min_\eta L_{\text{dual}} = \arg \max_\eta \widehat{\mathbb{E}}[\log p_\eta(X|y)]$

2. Train prior and forward: Plug in η^*

$p^{\text{mix}}(X, y) = \frac{1}{1+\beta} \hat{p}(X, y) + \frac{\beta}{1+\beta} \hat{p}(y) p_{\eta^*}(X|y)$

$\gamma^*, \alpha^* = \arg \min_{\gamma, \alpha} L_{\text{dual}}$

$= \widehat{\mathbb{E}}_{p_{(X,y)}^{\text{mix}}}[\log p_\gamma(X) + \log p_\alpha(y|X)]$

[Test Phase]: Inference:

Input: $\theta^* = \{\gamma^*, \alpha^*, \eta^*\}$, y^{test} , Proposal P .

$L \leftarrow P(y^{\text{test}})$

$X^* = \arg \min_{X \in L} E_{\theta^*}(X, y^{\text{test}})$

Return X^*

and Fig 4 in Appendix). Here is our training procedure. Since we parameterize the three probabilities separately, the optimization of dual loss breaks into two steps:

- **Step 1: Train backward.** η does not depend on forward direction under empirical data distribution. $\eta^* = \arg \min_{\eta} L_{\text{dual}} = \arg \max_{\eta} \widehat{E}[\log p_{\eta}(X|y)]$. η can be learned by MLE.
 - **Step 2: Train prior and forward.** We plug η^* into $p_{\eta^*}^{\text{mix}}(X, y)$. $\gamma^*, \alpha^* = \arg \min_{\gamma, \alpha} L_{\text{dual}} = \arg \max_{\gamma, \alpha} \widehat{\mathbb{E}}_{p_{\eta^*}^{\text{mix}}(X, y)}[\log p_{\gamma}(X) + \log p_{\alpha}(y|X)]$. γ, α can be learned by MLE.
- We provide ablation study of each component of dual loss in Appendix 5.4. The results show that each component in dual loss contribute to the final performance positively.

2.1.4 Perturbed model

In contrast to the ordered model that factorizes the sequence in one direction, we use a perturbed sequential model to achieve stochastic bidirectional factorization adapted from XLNet [23]. In particular, this model permutes the factorization order (while maintaining position encoding of the original order) that is used in the forward autoregressive model.

$$p(X|y, z) = p(X^{(z_1)}, X^{(z_2)}, \dots, X^{(z_{|s(X)|})}|y) = \prod_{i=1}^{|s(X)|} p_{\theta}(X^{(z_i)}|X^{(z_1:z_{i-1})}, y) \quad (12)$$

where the permutation order z is a permutation of the original order sequence $z_o = [1, 2, \dots, |X|]$ and z_i denotes the i -th element of permutation z . Here z is treated as hidden variable.

2.1.5 Bidirectional model

An alternative way to achieve bidirectional context conditioning is the denoising auto-encoding model. We adapt bidirectional model from BERT [24] to our application. The conditional probability $p(X|y)$ is factorized into product of conditional distributions of one random variable conditioning on others,

$$p(X|y) \approx \exp\left(\sum_{i=1}^{|s(X)|} \log p_{\theta}(X^{(i)}|X^{\neg i}, y)\right) \quad (13)$$

As presented in Wang and Cho [25], although the model is similar to MRF [26], the marginal of each dimension in Eq (13) does not have a simple form as in BERT training objective. It may result in a mismatch between the model and the learning objective. This model can be trained by pseudo-likelihood (Sec 3.2)

2.2 Graph-based Model

Compared with the sequence-based model, the graph-based methods present chemical molecules, with vertices as atoms and edges as chemical bonds. This natural parameterization allows straightforward application of chemistry knowledge by sub-graph matching with templates or reaction centers. We instantiated three representative graph-based approaches, namely NeuralSym [27], GLN [28] and G2G [15], from the framework. Firstly, we introduce an important concept *template*, which can assist modeling, learning, and inference.

Templates are reaction rules extracted from existing reactions. They are formed by reaction centers (a set of atoms changed, e.g. to form or break bonds). A template T consists of a product-subgraph pattern (t_y) and reactants-subgraph pattern(s) (t_X), denoted as $T := t_y \rightarrow t_X$, where X is a molecular set. We overload the notation to define a *template operator* $T(\cdot) : M \mapsto \mathcal{P}(M)$ which takes a product as input, and returns a set of candidate reactant sets. $T(\cdot)$ works as follows: enumerate all the templates with product-subgraph t_y matching with the given product y and define $S(y) = \{T : t_y \in y, \forall T \in \mathcal{T}\}$, where \mathcal{T} are available templates; then reconstruct the reactant candidates by instantiating reactant-subgraphs of the matched templates $R = \{X : t_X \in X, \forall T \in S(y)\}$. The output of $T(\cdot)$ is R . $T(\cdot)$ can be implemented by chemistry toolbox RDKit [29].

2.2.1 Template prediction: NeuralSym

NeuralSym is a template-based method, which treats the template prediction as multi-class classification. The corresponding probability model under the EBM framework can be written as:

$$p(X|y) \propto \sum_{T \in \mathcal{T}} \exp(e_T^\top f(y)) \mathbb{I}[X \in T(y)] \quad (14)$$

where $f(\cdot)$ is a neural network that embeds molecule graph y , and e_T is the embedding of template T . Learning such model requires only optimizing the cross entropy, despite that the number of potential templates could be very large.

2.2.2 Graph-matching with template: GLN

Dai et al. [28] proposed a method of graph matching the reactants and products with their corresponding components in the template to model the reactants and template jointly, with the model:

$$p(X, T|y) \propto \exp(w_1(T, y) + w_2(X, T, y)) \cdot \phi_y(T) \phi_{y, T}(X) \quad (15)$$

where w_1 and w_2 are graph matching score functions, and the $\phi(\cdot)$ operators defines the hard template matching results. This model assigns zero probability to the reactions that do not match with the template. $p(X|y)$ can be obtained by marginalizing over all templates.

2.2.3 Graph matching with reaction centers, G2G and GraphRETRO

In contrast with GLN, a few recent works G2Gs [15] and GraphRETRO [17] proposed to predict reaction center directly. These methods closely imitate chemistry experts when performing retrosynthesis: first identify reaction centers (i.e. where the bond breaks, denoted as c), then reconstruct X .

$$p(X|y) \propto \exp\left(\log\left(\sum_{c \in \mathcal{C}_y} p(X|c, y) p(c|y)\right)\right) \quad (16)$$

All the methods mentioned above require the additional atom-mapping as supervision during training, while NeuralSym and GLN require template information during inference. So NeuralSym and GLN are template-based methods. Since atom mapping plus reaction centers have almost same information as templates, we denote G2G and GraphRETRO method as semi-template-based approach.

3 Learning

Training EBMs is to learn parameters θ . In particular, we introduce three ways to learn exact (if applicable) or approximate maximum likelihood estimation (MLE) for full energy-based model (Sec 2.1.1), as this model includes other sequence-based EBM variants (ordered, perturbed, bidirectional, etc) by instantiating E_θ accordingly. Training EBMs with MLE is non-trivial because the partition function $Z(\theta)$ in Eq (1) is generally intractable. Computing $Z(\theta)$ involves approximation or additional information.

3.1 Approximate MLE: integration using template.

We use additional chemistry information: Templates. Direct MLE is not feasible because the partition function of Eq (3) involves enumerating full molecular set M , which is intractable. Here we use templates to get a finite support of the partition function. Specifically, we use template operator to extract a set of reactant candidates associated with y , denoted as $T(y)$. As the size of $T(y)$ is about tens to hundreds (not computationally prohibitive), we can perform exact inference of Eq (3) to obtain the MLE. We denote this training scheme as *template learning*.

3.2 Approximate MLE: pseudo-likelihood.

Alternatively, we can provide an approximation of Eq (3) via pseudo-likelihood [30] to enable training. Pseudo-likelihood factorizes the joint distribution into the product of conditional probabilities of each variable given the rest. Theoretically, the pseudo-likelihood estimator yields an exact solution if the data is generated by a model $p(X|y)$ and number of data points $n \rightarrow \infty$ (i.e., it is consistent) [30]. For the full model, training is performed as:

$$p(X|y) \approx \exp\left(\sum_{i=1}^{|s(X)|} \log p_\theta(X^{(i)}|X^{-i}, y)\right) = \exp\left(\sum_i^{|s(X)|} \log \frac{\exp(g_\theta(X, y))}{\sum_{c \in \mathcal{S}} \exp(g_\theta(X', y; X'^{-i} = X^{-i}, X'^{(i)} = c))}\right) \quad (17)$$

where the superscript \neg indicates sequence except the i -th token and $g_\theta(p, q) : S^{|p|} \times S^{|q|} \mapsto \mathbb{R}$ is a transformer architecture that maps two sequences to a scalar. As bidirectional model Sec 2.1.5

and training approaches Sec 3.2 (approximate joint probability) factorizes in the same way, pseudo-likelihood is a convenient way to train this model.

3.3 Exact MLE: tractable factorization.

This training procedure works for a special case of the full model, which has a tractable factorization of the joint probability, e.g., autoregressive models in ordered (Sec 2.1.2) and perturbed (Sec 2.1.4).

3.4 Generalized sequence model.

Generalized sequence model first infer latent variable $S^* = \arg \max p(S|y)$ and then infer $X^* = \arg \max p(X|y, S^*)$ as the vanilla sequence-based model with S provided as additional input (e.g. concatenate S^* and y).

4 Inference

With the trained E_{θ^*} , inference identifies the best X that minimizes the energy function for given y^{test} , i.e. $X^{\text{test}} = \arg \min_{X \in \mathcal{X}} E_{\theta^*}(X, y^{\text{test}})$. Directly solving the above minimization is again intractable, but the energy function can generally be used for ranking. Let R denote the rank of candidate X_i for the given y^{test} (lower is better).

$$\{R(X_1) < R(X_2) \iff E_{\theta^*}(X_1, y^{\text{test}}) < E_{\theta^*}(X_2, y^{\text{test}})\} \quad (18)$$

Practically, as illustrated in Fig 2, one can use either template-based or template-free method to come up with initial proposals for ranking, as follows.

Template-based Proposing (TB). Templates can be used to extract a list of proposed reactant candidates by using templates. We use template operator $T(\cdot)$ (defined in Sec 2.2) to propose a list of candidate reactant sets from the input product y . **Template-free Proposing (TF).** In this paper, *template-free ranking* makes proposals using the learned prediction model. We use a simple autoregressive form for $p(X|y)$ (Ordered model), which can draw the top K most likely samples from this distribution using beam search, which is computational efficient.

5 Experiments

5.1 Experiment setup

Dataset and evaluation used follow existing work [31, 28, 13, 15]. We evaluate our method on a benchmark dataset named USPTO-50k, which includes 50k reactions falling into ten reaction types from the US patent literature. The datasets are split into train/validation/test with percentage of 80%/10%/10%. Our evaluation metric is the top- k exact match accuracy, referring to the percentage of examples where the ground truth reactant set was found within the top k predictions made by the model. Following the common practice, we use RDKit [29] to canonicalize the SMILES string. For sequence-based models, we incorporate the augmentation trick to ensure best performance. The procedures are as follows: (1) Replace each molecule in reactant set or product using random SMILES; (2) Random permute the order of reactant molecules. The augmented SMILES are different linearizations of the same molecules. It can prevent sequence-based models (transformer) from over-fitting. However, the augmentation does not improve performance for graph-based models, as graph-based models take graph format as input which is invariant for different augmentations.

5.2 Existing methods

We evaluate of our approach against several existing methods, including both template-based, semi-template based and template-free approaches. **Template-free methods:** Transformer [14] is a transformer based approach that trains a second transformer to identify the wrong translations and remove them. LSTM [13] is a sequence to sequence approach that use LSTM as encoder and decoder. **Template-based methods:** retrosim [31] selects template for target molecules using fingerprint based similarity measure between targets and templates; neuralysm [27] performs selection of templates as a multiple-class problem using MLP; GLN builds a template induced graphical model and makes prediction with approximated MAP.

Semi-Template based methods: G2Gs [15], GRetroXpert [16], and GraphRETRO [17] share the same idea: infer reaction center to generate synthons, and then complete the missing pieces (aka "leaving groups") in synthons to generate reactants. These methods use "reaction centers" as additional information to supervise their algorithm. The reaction centers preserve key information in templates. So we denote them as "Semi-Template".

5.3 Template-free evaluation

Table 1 shows our best EBM variant (the dual model) evaluated in a template free setup. We first perform evaluations on all the EBM variants introduced in Sec 2.1 to select the best EBM variant. The results show that the dual model outperforms other EBM variants by a clear margin (Table 4 in Appendix). The evaluation is on template-based proposing to ensure the proposal list of candidate molecules is the same for all the variants.

Then we pursue further on template-free setup. An ideal model requires a proposal model with good coverage and a ranking model with good accuracy. We explored various combinations of proposal-ranking pairs. The proposal model evaluated is the ordered model trained on USPTO50K and augmented USPTO50K, respectively. The ranking model is the dual model trained on augmented data, as it performs the best in Table 4. Our best performer is ordered-proposal (USPTO 50K)-dual-ranking (aug USPTO 50K) model. A case study showing how dual model improves accuracy upon proposal is given in Fig 3, where it shows how the energy based re-ranking refines the initial proposal. One interesting observation is that, the proposal ordered model trained on augmented data has higher top 1 accuracy but much lower top 10 accuracy, than the one trained without augmentation. This indicates that the proposal using augmented data has low coverage in the prediction space. We observed that the model learned on augmented dataset learns various representations of the same molecule (due to usage of random SMILES). A certain percentage of proposed candidates are the same after canonicalization, which is good for top 1 prediction during ranking but undesired for proposal.

Table 1: **Template-free: Dual model:** Translation Proposal and Dual Ranking

Type	Proposal					Re-rank					
	Proposal model	Top 1	Top 5	Top 10	Top 50	Top 100	Rank model	Top 1	Top 3	Top 5	Top 10
No	Ordered on UPSPTO	44.4	64.9	69.9	77.2	78.0	Dual trained on Aug USPTO	53.6	70.7	74.6	77.0
	Ordered on Aug USPTO	53.2	54.7	55.6	60.5	60.5	SOTA (RetroXpert [16])	54.5	60.0	60.4	60.5
	-	-	-	-	-	-	-	50.4	61.1	62.3	63.4
Yes	Ordered on USPTO	56.0	76.1	79.7	85.2	86.4	Dual trained on Aug USPTO	65.7	81.9	84.7	85.9
	Ordered on Aug USPTO	64.7	66.5	67.3	69.7	75.7	SOTA (RetroXpert [16])	66.2	75.1	75.6	75.7
	-	-	-	-	-	-	-	62.1	75.8	78.5	80.9

5.4 Ablation Study of the dual loss

Since the dual variant serves as the backbone variant in the previous section, we perform additional ablation study to investigate the performance of the dual variant with respect to different designs of the dual loss. Table 2 shows that each component of the dual loss contribute positively to the final performance. The dual constraint leads to additional improvement on the top of other components, which is more challenging to achieve in a higher accuracy region.

The evaluation of Table 2 is under the same setup as Table 4 – uses template-based proposal for fair and easy comparison. The notations of Table 2 are as follows: The "dual" row are entries taken from Table 4, showing results trained with dual loss. To recap, the dual loss is defined in Eq (10) and the dual constraint is its middle term. $\widehat{\mathbb{E}}[\log p_\gamma(X) + \log p_\alpha(y|X) + \log p_\eta(X|y)]$ is the dual loss without the dual constraint. $\widehat{\mathbb{E}}[\log p_\alpha(y|X) + \log p_\eta(X|y)]$ is the dual loss without the prior $\log p_\gamma(X)$. $\log p_\eta(X|y)$ is only including backward direction.

Table 2: **Ablation Study of dual loss design when reaction type is known**

Aug USPTO	Top 1	Top 3	Top 5	Top 10
Dual	67.7	84.8	88.9	92.0
$\widehat{\mathbb{E}}[\log p_\gamma(X) + \log p_\alpha(y X) + \log p_\eta(X y)]$	67.0	84.7	88.9	91.95
$\widehat{\mathbb{E}}[\log p_\alpha(y X) + \log p_\eta(X y)]$	66.1	82.8	87.6	91.3
$\widehat{\mathbb{E}}[\log p_\eta(X y)]$	60.9	80.9	85.8	90.2

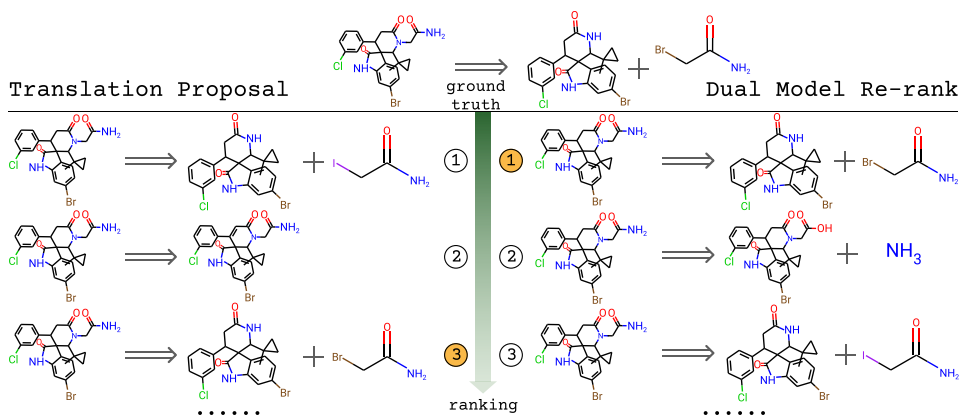


Figure 3: **Dual ranking improves upon translation proposal.** Left and right column are the top three candidates from translation proposal and dual re-ranking of the proposal. Ground truth (GT) is given at the top and is labeled orange in the middle. By dual re-ranking, the GT ranks the first place, whereas the 3rd place in the proposal. Note that the first place in the proposal is only one atom different from GT (Br vs I), indicating the dual model is able to identify small changes in structure. Another example is given in Fig 5 in Appendix.

Table 3: **Top K exact match accuracy** of existing methods

Category	Model	Reaction type unknown				Reaction type known			
		top1	top3	top5	top10	top1	top3	top5	top10
TB	retrosim [31]	37.3	54.7	63.3	74.1	52.9	73.8	81.2	88.1
	NeuralSym [27]	44.4	65.3	72.4	78.9	55.3	76.0	81.4	85.1
	GLN [28]	52.5	69.0	75.6	83.7	64.2	79.1	85.2	90.0
Semi-TB	G2Gs [15]	48.9	67.6	72.5	75.5	61.0	81.3	86.0	88.7
	GraphRETRO [17]	53.7	68.3	72.2	75.5	63.9	81.5	85.2	88.1
	RetroXpert [16]	50.4	61.1	62.3	63.4	62.1	75.8	78.5	80.9
TF	LSTM [13]	-	-	-	-	37.4	52.4	57.0	61.7
	Transformer [14]	43.7	60.0	65.2	68.7	59.0	74.8	78.1	81.1
	Dual (Ours)	53.6	70.7	74.6	77.0	65.7	81.9	84.7	85.9

5.5 Comparison against the state-of-the-art

Table 3 presents the main results. All the baseline results are extracted from existing works as we share the same experiment protocol. The dual model is trained with randomized SMILES to inject order invariance information of molecule graph traversal. Note that other methods like graph-based variants do not require such randomization as the graph representation is already order invariant. We can see that, regarding top 1 accuracy, our proposed dual model outperforms the current state-of-the-art methods. Semi-template methods are those require ground truth reaction centers during training as supervision, whereas generalized dual model does not require this additional information, yet still output perform the best semi-template models by 1.6% when reaction type is known. This demonstrates the advantages of the dual model. RetroXpert results are the updated results taken from <https://github.com/uta-smile/RetroXpert>.

6 Conclusion

In this paper we proposed an unified EBM framework that integrates multiple sequence- and graph-based variants for retrosynthesis. Assisted by a comprehensive assessment, we provide a critical understanding of different designs. Based on this, we proposed a novel variant – generalized dual model, which outperforms state-of-the-art in template free manner.

References

- [1] EJ Corey. Robert robinson lecture. retrosynthetic thinking—essentials and examples. *Chemical Society Reviews*, 17:111–133, 1988.
- [2] Elias James Corey. The logic of chemical synthesis: multistep synthesis of complex carbogenic molecules (nobel lecture). *Angewandte Chemie International Edition in English*, 30(5):455–465, 1991.
- [3] Marwin HS Segler, Mike Preuss, and Mark P Waller. Planning chemical syntheses with deep neural networks and symbolic ai. *Nature*, 555(7698):604–610, 2018.
- [4] Sara Szymkuć, Ewa P Gajewska, Tomasz Klucznik, Karol Molga, Piotr Dittwald, Michał Startek, Michał Bajczyk, and Bartosz A Grzybowski. Computer-assisted synthetic planning: The end of the beginning. *Angewandte Chemie International Edition*, 55(20):5904–5937, 2016.
- [5] Felix Strieth-Kalthoff, Frederik Sandfort, Marwin HS Segler, and Frank Glorius. Machine learning the ropes: principles, applications and directions in synthetic chemistry. *Chemical Society Reviews*, 49(17):6154–6168, 2020.
- [6] Connor W Coley, Regina Barzilay, Tommi S Jaakkola, William H Green, and Klavs F Jensen. Prediction of organic reaction outcomes using machine learning. *ACS central science*, 3(5): 434–443, 2017.
- [7] Connor W Coley, Dale A Thomas, Justin AM Lummiss, Jonathan N Jaworski, Christopher P Breen, Victor Schultz, Travis Hart, Joshua S Fishman, Luke Rogers, Hanyu Gao, et al. A robotic platform for flow synthesis of organic compounds informed by ai planning. *Science*, 365(6453): eaax1566, 2019.
- [8] Marwin HS Segler and Mark P Waller. Modelling chemical reasoning to predict and invent reactions. *Chemistry—A European Journal*, 23(25):6118–6128, 2017.
- [9] Simon Johansson, Amol Thakkar, Thierry Kogej, Esben Bjerrum, Samuel Genheden, Tomas Bastys, Christos Kannas, Alexander Schliep, Hongming Chen, and Ola Engkvist. Ai-assisted synthesis prediction. *Drug Discovery Today: Technologies*, 2020.
- [10] David Weininger. Smiles, a chemical language and information system. 1. introduction to methodology and encoding rules. *Journal of chemical information and computer sciences*, 28(1):31–36, 1988.
- [11] Ashish Vaswani, Noam Shazeer, Niki Parmar, Jakob Uszkoreit, Llion Jones, Aidan N Gomez, Łukasz Kaiser, and Illia Polosukhin. Attention is all you need. In *Advances in neural information processing systems*, pages 5998–6008, 2017.
- [12] Philippe Schwaller, Teodoro Laino, Théophile Gaudin, Peter Bolgar, Christopher A Hunter, Costas Bekas, and Alpha A Lee. Molecular transformer: A model for uncertainty-calibrated chemical reaction prediction. *ACS central science*, 5(9):1572–1583, 2019.
- [13] Bowen Liu, Bharath Ramsundar, Prasad Kawthekar, Jade Shi, Joseph Gomes, Quang Luu Nguyen, Stephen Ho, Jack Sloane, Paul Wender, and Vijay Pande. Retrosynthetic reaction prediction using neural sequence-to-sequence models. *ACS central science*, 3(10): 1103–1113, 2017.
- [14] Shuangjia Zheng, Jiahua Rao, Zhongyue Zhang, Jun Xu, and Yuedong Yang. Predicting retrosynthetic reactions using self-corrected transformer neural networks. *Journal of Chemical Information and Modeling*, 2019.
- [15] Chence Shi, Minkai Xu, Hongyu Guo, Ming Zhang, and Jian Tang. A graph to graphs framework for retrosynthesis prediction. *arXiv preprint arXiv:2003.12725*, 2020.
- [16] Chaochao Yan, Qianggang Ding, Peilin Zhao, Shuangjia Zheng, Jinyu Yang, Yang Yu, and Junzhou Huang. Retroxpert: Decompose retrosynthesis prediction like a chemist. 2020.

- [17] Vignesh Ram Somnath, Charlotte Bunne, Connor W Coley, Andreas Krause, and Regina Barzilay. Learning graph models for retrosynthesis prediction. *arXiv preprint arXiv:2006.07038*, 2020.
- [18] Yann LeCun, Sumit Chopra, Raia Hadsell, M Ranzato, and F Huang. A tutorial on energy-based learning. *Predicting structured data*, 1(0), 2006.
- [19] Geoffrey E Hinton. A practical guide to training restricted boltzmann machines. In *Neural networks: Tricks of the trade*, pages 599–619. Springer, 2012.
- [20] Ilya Sutskever, Oriol Vinyals, and Quoc V Le. Sequence to sequence learning with neural networks. In *Advances in neural information processing systems*, pages 3104–3112, 2014.
- [21] Di He, Yingce Xia, Tao Qin, Liwei Wang, Nenghai Yu, Tie-Yan Liu, and Wei-Ying Ma. Dual learning for machine translation. In *Advances in neural information processing systems*, pages 820–828, 2016.
- [22] Bolin Wei, Ge Li, Xin Xia, Zhiyi Fu, and Zhi Jin. Code generation as a dual task of code summarization. In *Advances in Neural Information Processing Systems*, pages 6559–6569, 2019.
- [23] Zhilin Yang, Zihang Dai, Yiming Yang, Jaime Carbonell, Russ R Salakhutdinov, and Quoc V Le. Xlnet: Generalized autoregressive pretraining for language understanding. In *Advances in neural information processing systems*, pages 5754–5764, 2019.
- [24] Jacob Devlin, Ming-Wei Chang, Kenton Lee, and Kristina Toutanova. Bert: Pre-training of deep bidirectional transformers for language understanding. *arXiv preprint arXiv:1810.04805*, 2018.
- [25] Alex Wang and Kyunghyun Cho. Bert has a mouth, and it must speak: Bert as a markov random field language model. *arXiv preprint arXiv:1902.04094*, 2019.
- [26] Ross Kindermann. Markov random fields and their applications. *American mathematical society*, 1980.
- [27] Marwin HS Segler and Mark P Waller. Neural-symbolic machine learning for retrosynthesis and reaction prediction. *Chemistry—A European Journal*, 23(25):5966–5971, 2017.
- [28] Hanjun Dai, Chengtao Li, Connor Coley, Bo Dai, and Le Song. Retrosynthesis prediction with conditional graph logic network. In *Advances in Neural Information Processing Systems*, pages 8870–8880, 2019.
- [29] G Landrum. Rdkit: Open-source cheminformatics software, 2016.
- [30] Julian Besag. Statistical analysis of non-lattice data. *Journal of the Royal Statistical Society: Series D (The Statistician)*, 24(3):179–195, 1975.
- [31] Connor W Coley, Luke Rogers, William H Green, and Klavs F Jensen. Computer-assisted retrosynthesis based on molecular similarity. *ACS central science*, 3(12):1237–1245, 2017.
- [32] Andrew Dalke. Deepsmiles: An adaptation of smiles for use in. 2018.
- [33] Mario Krenn, Florian Häse, AkshatKumar Nigam, Pascal Friederich, and Alán Aspuru-Guzik. Selfies: a robust representation of semantically constrained graphs with an example application in chemistry. *arXiv preprint arXiv:1905.13741*, 2019.
- [34] Guillaume Klein, Yoon Kim, Yuntian Deng, Jean Senellart, and Alexander M Rush. Opennmt: Open-source toolkit for neural machine translation. *arXiv preprint arXiv:1701.02810*, 2017.
- [35] Diederik P Kingma and Jimmy Ba. Adam: A method for stochastic optimization. *arXiv preprint arXiv:1412.6980*, 2014.

A Appendix

A.1 Terminology: Reaction center and Synthons

Reaction center of a chemical reaction are the bonds that are broken or formed during a chemical reaction. For retrosynthesis, reaction centers are bonds exist in product, but do not exist in reactants. One chemical reaction may have multiple reaction centers. Synthons are the sub-parts extracted from the products by breaking the bonds in the reaction center. Synthons are usually not valid molecules with * to indicate the broken ends in the reaction centers.

A.2 Sequence-based variant evaluation

In this section, we mainly compare different energy based sequence models described in Sec 2.1. Table 4 provides the results of each sequence model variant described in Sec 2.1. For simplicity of the proposal, we evaluate them using *template-based ranking* described in Sec 4. Each variant is evaluated on USPTO 50K and augmented USPTO 50K using random SMILES.

Without reiterating good performance for the dual variant, we focus on discussion of variants with undesired performance. The perturbed sequential model (Sec 2.1.4) and bidirectional model (Sec 2.1.5) are inferior to dual or ordered models, where the main reason possibly comes from the fact that the learning objective approximates the actual model and Eq (13) poorly, and thus leads to discrepancy between training and inference. The full model (Sec 2.1.1) despite being most flexible and achieving best top 10 performance when type is given, would suffer from high computation cost due to the explicit integration even with the templates. In addition to the understanding of individual models throughout the comprehensive study, we find it is important to balance the trade-off between model capacity and learning tractability. A powerful model without effective training would be even inferior to some well trained simple models. Our dual model makes a good balance between capacity and learning tractability.

Table 4: Ablation study: Top K accuracy of sequence variants

Models	Reaction type unknown				Reaction type known			
	Top 1	Top 3	Top 5	Top 10	Top 1	Top 3	Top 5	Top 10
Ordered	54.2	72.0	77.7	84.2	66.4	82.9	87.4	91.0
Perturbed	47.3	64.6	70.4	75.8	64.2	79.8	83.3	86.4
Bidirectional	23.5	43.7	54.3	69.5	41.9	66.3	75.6	84.6
Dual	55.2	74.6	80.5	86.9	67.7	84.8	88.9	92.0

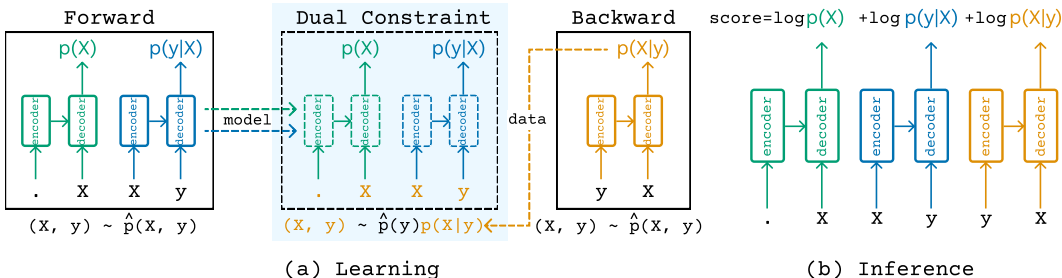


Figure 4: **Dual model.** (a) **Learning** consists of training three transformers: prior $p(X)$ (green), likelihood $p(y|X)$ (blue), and backward $p(X|y)$ (orange). Dual model penalizes the divergence between forward $p(X)p(y|X)$ and backward direction $p(y|X)$ with Dual constraint (highlighted). (b) **Inference** Given reactant candidates list, we rank them using Eq (7).

A.3 Time and space complexity analysis

In this section, we provide time and space complexity regarding model design choices. As the main bottleneck is the computation of transformer model, we measure the complexity in the unit

of transformer model calls. For all the models, the inference only requires the evaluation of (un-normalized) score function, thus the complexity is $O(1)$; For training, the methods that factored have an easy form of likelihood computation, where a diagonal mask is applied to input sequence so that autoregressive is done in parallel (not $|s(x)|$ times), so it requires $O(1)$ model calls. This include ordered/perturbed/bidirectional/dual models. For the full model trained with pseudo-likelihood, it requires $O(|X| \cdot |S|)$ calls due to the evaluation per each dimension and character in vocabulary. Things would be a bit better when trained with template-based method, in which it requires $O(|T(y)|)$ calls, which is proportional to the number of candidates after applying template operator.

As the memory bottleneck is also the transformer model, it has the same order of growth as time complexity with respect to sequence length and vocabulary size. In summary we can see the Full model has much higher cost for training, which might lead to inferior performance. Our dual model with a consistency training objective has the same order of complexity than other autoregressive ones, while yields higher capacity and thus better performance.

A.4 Example of case study

Here we provide another case study showing with dual model ranking (Sec 2.1.3), the accuracy improves upon translation proposal. Please see Fig 3 and Fig 5.

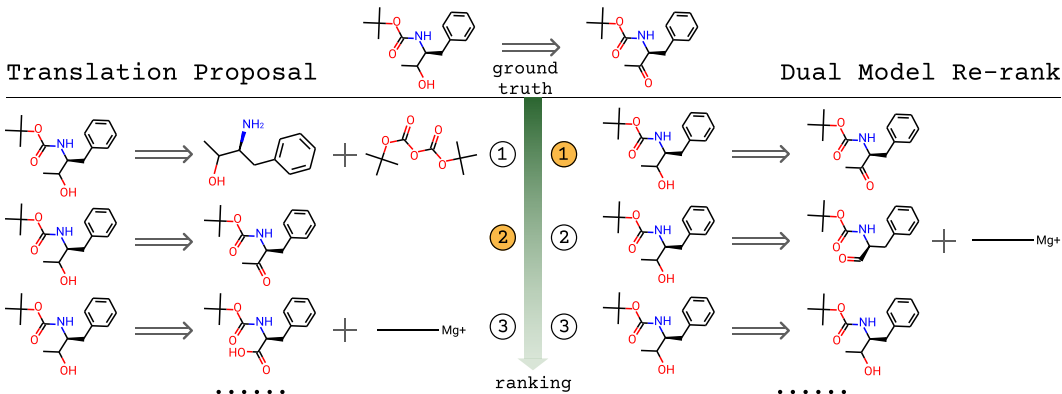


Figure 5: **Dual ranking improves upon translation proposal.** Another example. Descriptions see Fig 3

A.5 Alternative of SMILES: deepSMILES and SELFIES

In this section, we explore the effect of preprocessing procedure of sequence-based model, e.g. inline representation of molecular graph, in effecting performance of sequence-based model. In particular, deepSMILES [32] and SELFIES [33] are alternatives to SMILES. Without loss of fairness, we evaluated these representations using Ordered sequential model (Sec 2.1.2). The results indicate SMILES work the best. We speculate the reason are deepSMILES and SELFIES are on average longer than SMILES, leading to higher probability of making mistakes on token level and therefore low sequence-level accuracy.

A.6 Transformer implementation of Permutation Invariant of reactant set

Transformer has a position encoding to mark the different locations on an input sequence. We modified the position encoding such that each molecule starts with 0 encoding, instead of the concatenated position in the reactants sequence. The results are Table 6. We can see that this position encoding is beneficial for non-augment data, but not augment data, as the latter has already considered the permutation invariance order of reactants by data augmentation. In this paper, we use data augmentation to maintain order-invariant for reactants.

Table 5: **deepSMILES and SELFIES**

SMILES				
Models	Top 1	Top 3	Top 5	Top 10
Ordered	47.0	67.4	75.4	83.1
deepSMILES				
Ordered	46.08	65.87	73.54	81.51
Selfies				
Ordered	43.00	62.51	70.16	79.07

Table 6: **Transformer model with permutation invariant position encoding**

Reaction type is unknown	USPTO 50k				
Models	Top 1	Top 2	Top 3	Top 5	Top 10
Ordered	46.97	60.71	67.39	75.35	83.14
Ordered + Permutation invariant	47.29	61.29	68.08	75.37	83.36
Augmented data					
Ordered	54.24	66.33	72.02	77.67	84.22
Ordered + Permutation invariant	53.45	66.61	72.58	78.33	85.42

A.7 Discussion

V.1 Full model (Sec 2.1.1) Full model (Sec 2.1.1) with template learning reaches accuracy of 39.5% and 53.7% on USPTO50k data-sets. Full model is partially limited by expensive computation due to the number of candidates per product.

V.2 Perturbed sequential model (Sec 2.1.4) During training, permutation order z is randomly sampled and

uses the following training objective:

$$p(X|y) \approx \exp \left(\mathbb{E}_{z \sim Z_{|s(x)|}} \left[\sum_{i=1}^{|X|} \log p_{\theta}(X^{(z_i)} | z_i, X^{(z_1:z_{i-1})}, y) \right] \right) \quad (19)$$

and the corresponding parameterization:

$$p_{\theta}(X^{(z_i)} | z_i, X^{(z_1:z_{i-1})}, y) = \log \frac{\exp(h(X^{(z_1:z_{i-1})}, z_i, y)^{\top} e(X^{z_i}))}{\sum_{c \in S} \exp(h(X^{(z_1:z_{i-1})}, z_i, y)^{\top} e(c))} \quad (20)$$

where z_i encodes which position index in the permutation order to predict next, implemented by a second position attention (in addition to the primary context attention). Note that Eq (19) is actually a lower bound of the latent variable model, due to Jensen’s inequality. However, we focus on this model design for simplicity of permuting order in training.

The lower-bound approximation is tractable for training. Perturbed sequential model has about $\sim 4\%$ accuracy loss in top 1 accuracy compared with ordered model (Sec 2.1.2). We argue the reason are as follows: firstly, we designed E_{θ} as the middle term of Eq (19) to facilitate perturbing the order during training, following [23]. However, due to Jensen’s inequality, this design is not equal to $P(X|y)$, which causes discrepancy in ranking (inference).

V.3 Bidirectional model (Sec 2.1.5)

Bidirectional model, however, does not perform well in our experiments. The bidirectional-awareness makes the prediction of one position given all the rest of the sequence $p(X^{(i)}|X^{-i}, y)$ almost perfect (99.9% accuracy in token-level). However, due to the gap between pseudo-likelihood and maximum likelihood, *i.e.*, $\log P(X|y)$, the performance for predicting the whole sequence will be inferior, as we observed in the experiments.

A.8 Transformer architecture and training details

The implementation of variants in framework is based on OpenNMT-py [34]. Following [11], transformer is implemented as encoder and decoder, each has a 4 self-attention layers with 8 heads and a feed-forward layer of size 2048. We use model size and word embedding size as 256. Batch size contains 4096 tokens, which approximately contains 20-200 sequences depending on the length of sequence. We trained for 500K steps, where each update uses accumulative gradients of four batches. The optimization uses Adam [35] optimizer with $\beta_1 = 0.9$ and $\beta_2 = 0.998$ with learning rate described in [11] using 8000 warm up steps. The training takes about 48 hours on a single NVIDIA Tesla V100. The setup is true for training transformer-based models, including ordered sequential model (Sec 2.1.2), perturbed sequential model (Sec 2.1.4), bidirectional model (Sec 2.1.5), dual model (Sec 2.1.3). As for full model (Sec 2.1.1), each sample contains 20-500 candidates. We implemented as follows: each batch only contains one sample. Its tens or hundreds of candidates are computed in parallel within the batch. The model parameters are updated when accumulating 100 batches to perform one step of update.